Journal of Experimental Nanoscience
Publication details, including instructions for authors and subscription information:
http://www.informaworld.com/smpp/title~content=t716100757

Electron spin resonance in silver-doped PbS nanorods

A. R. Mandal[a]; S. K. Mandal[a]
[a] Department of Physics, Visva-Bharati, Santiniketan 731 235, West Bengal, India

First published on: 15 March 2010

To cite this Article Mandal, A. R. and Mandal, S. K.(2010) 'Electron spin resonance in silver-doped PbS nanorods', Journal of Experimental Nanoscience, 5: 3, 189 — 198, First published on: 15 March 2010 (iFirst)
To link to this Article: DOI: 10.1080/17458080903464082
URL: http://dx.doi.org/10.1080/17458080903464082

Journal of Experimental Nanoscience
Vol. 5, No. 3, June 2010, 189–198

Electron spin resonance in silver-doped PbS nanorods

A.R. Mandal and S.K. Mandal*

Department of Physics, Visva-Bharati, Santiniketan 731 235, West Bengal, India

(*Received 25 November 2008; final version received 4 November 2009*)

The electron spin resonance characteristics of silver (Ag)-doped PbS nanorods have been investigated here. We show that both Ag^0 and Ag^{2+} centres can be simultaneously created in PbS nanorod structures grown in polymers. Structural investigations reveal that strain-induced distortion of PbS lattice can lead to the formation of hole traps in as-grown samples. Large strain-induced binding of the Ag^+ ions into the Pb^{2+} vacancies lowers the activation energy of diffusion significantly. The isomorphic substitution of Ag^+ in PbS host is then converted into Ag^0 and Ag^{2+} paramagnetic centres to maintain the charge neutrality and cation–anion ratio, confirmed by electron spin resonance investigations.

Keywords: PbS nanorods; silver doping; paramagnetic centre; ESR

1. Introduction

Creation of paramagnetic centres in semiconductors is of great fundamental interest over the years and has led to many exciting findings in physics. Besides, these paramagnetic ion-doped semiconductors are potentially attractive materials for various optical and magnetic devices, of late in spintronic devices [1–5]. Although paramagnetic ion doping in various II–VI and IV–VI semiconductors has been studied [6–8], creation of silver (Ag) paramagnetic centres and determination of their valence state in PbS (galena) are scarcely addressed [9]. The occurrence of pure metallic silver in galena is also very rare in nature. Simple substitution of Ag^+ in PbS ($2Ag^+ = Pb^{2+}$) through solid-state reaction is limited to only 0.4 mol% at 615°C [10,11]. The diffusion coefficient of silver in PbS is found to be very low, approximately $10^{-10}\,cm^2\,s^{-1}$ at 500°C [12]. It is further observed that the silver uptake in PbS can be enhanced when substitution takes place accompanying other ions (Sb, Bi, etc.), like $Ag^+ + Sb^{3+} = 2Pb^{2+}$ forming diaphorite $Pb_2Ag_3Sb_3S_8$. The insolubility of Ag in PbS arises out of the fact that half of the silver atoms are isomorphically substituted in the interstitial site in PbS. Such a structural configuration is energetically unfavourable for stable existence of Ag and PbS. However, the thermodynamic data reveals that there exists a wide range of temperature and fugacity values in which Ag and PbS can stably coexist [13,14]. The basic objective of this report is to address the structural role of Ag in PbS host and their paramagnetic behaviours. We show here that in low-dimensional structures of PbS, here in the form of nanorods in polymer matrix, silver

---

*Corresponding author. Email: sk_mandal@hotmail.com

ISSN 1745–8080 print/ISSN 1745–8099 online

DOI: 10.1080/17458080903464082
http://www.informaworld.com

concentration in PbS can be increased to 1.76 mol%. Determination of the structural information of silver at low concentrations in the presence of matrix containing heavy element Pb seems to be a challenging task. Electron spin resonance (ESR) is found to be quite sensitive in revealing such information for magnetic elements, even if the elemental concentrations present in the matrix is low. Interestingly, we found the valence state of silver present in PbS to be Ag^0 and Ag^{2+}. Both Ag^0 and Ag^{2+} paramagnetic centres simultaneously coexist in PbS structure, as revealed by ESR spectrum, which are not reported before. Creation of both the paramagnetic centres is instigated by the formation of vacancies when PbS undergoes a strain-induced lattice distortion from cubic to tetragonal one, as discussed in the following sections.

2. Experimental

Single crystalline preferential growth of PbS nanorods in polymer (polypyrole) is mentioned in detail in our recent report [15]. Briefly, the procedure takes place by exchanging Pb^{2+} ions into the pyrrole and then reacting with S^2. Solutions of lead nitrate (purified, Loba Chemie, India) and sodium thiosulfate (Merck, India) dissolved in a mixture of ethanol (GR, Jiangsu Huaxi, China) and distilled water (2:1) are used as the precursors for lead and sulphur. Then different amounts of pyrrole monomer (SRL, India) are added into the lead solution under rapid stirring to obtain various pyrrole concentrations 5, 10 and 15 wt% in the solution, respectively. Sulphidation takes place under rapid stirring condition when sulphur-containing solution is added to the mixture of Pb^{2+} solution and pyrrole at a fixed temperature. In the precursors, the molar ratio of lead and sulphur is maintained as $Pb : S = 1:1$ to obtain the required stoichiometry in the derived lead sulphide embedded in polypyrrole. Addition of sulphur into the lead-containing solution results into the instantaneous formation of PbS precipitate within the polypyrrole matrix. The precipitate is washed in distilled water for three times, filtered and dried at room temperature in vacuum. Silver doping is accomplished by the replacement of Pb^{2+} by 5 mol% of Ag^+ in the starting solutions (using silver nitrate as the precursor). Here, we are concerned with four samples, S-1–S-4. The samples S-1 and S-2 contain PbS nanorods grown with 5 wt% of polypyrrole at 60°C, the first one is undoped and the latter being doped with silver. Samples S-3 and S-4 are silver doped, grown with polypyrrole concentration 10 wt% and 15 wt% at temperature 80°C, respectively. We find that the concentration of silver really doped in the PbS lattice largely differs from that of silver concentration in the starting solution. Energy dispersive X-ray analyses (EDAX) show that the concentration of silver really doped in the samples S-2, S-3 and S-4 are 0.58, 1.17 and 1.76 mol%, respectively.

3. Results and discussion

The structural characterisations of the nanorods done by using electron microscopy and XRD are given in Figures 1 and 2, respectively. The diameter (D) of nanorods (obtained from TEM) is found to increase with the increase in polymer concentrations: $D = 30$ nm for S-1 and S-2, 50 nm for S-3 and 80 nm for S-4, respectively. A representative SEM and TEM images of sample S-4 is given in Figure 1(a) and (b), respectively, indicating the growth of PbS nanorods. SEM also indicates the narrow size distribution of the

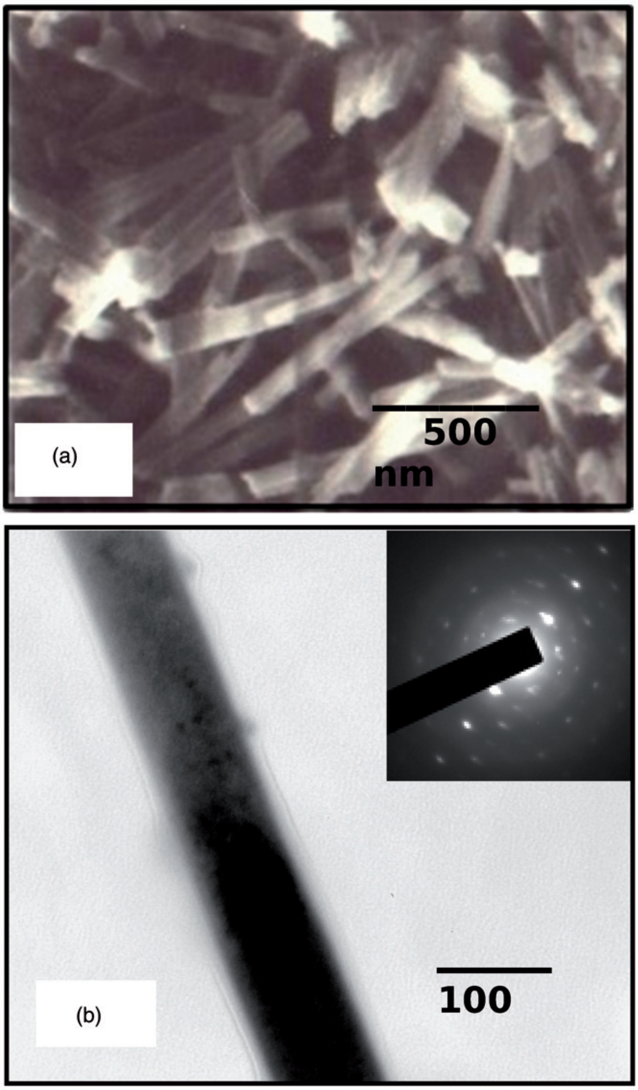

Figure 1. Representative (a) SEM and (b) TEM images showing the formation of nanorods of diameter approximately 80 nm. Inset of (b) shows the selected area diffraction pattern indicating single crystalline growth of nanorods.

nanorod sample. Inset of Figure 1(b) shows the corresponding selected area electron diffraction (SAED) pattern. The diffraction spots in SAED are clear, indicative of the single-crystalline growth of PbS nanorods in polymer. The XRD spectra (Figure 2) showing the shift in peak position (hence in lattice spacing d) compared to bulk indicate a strong lattice distortion. Further, we find a decrease in d spacing for the most intense (2 2 0) peak, while other peaks like (1 1 1) and (2 0 0) exhibit increase in d values. Considering the (2 2 0) plane, we calculate the lattice contraction by 2.77%. On the other hand, calculation based on (1 1 1) plane indicates an expansion of the lattice as large

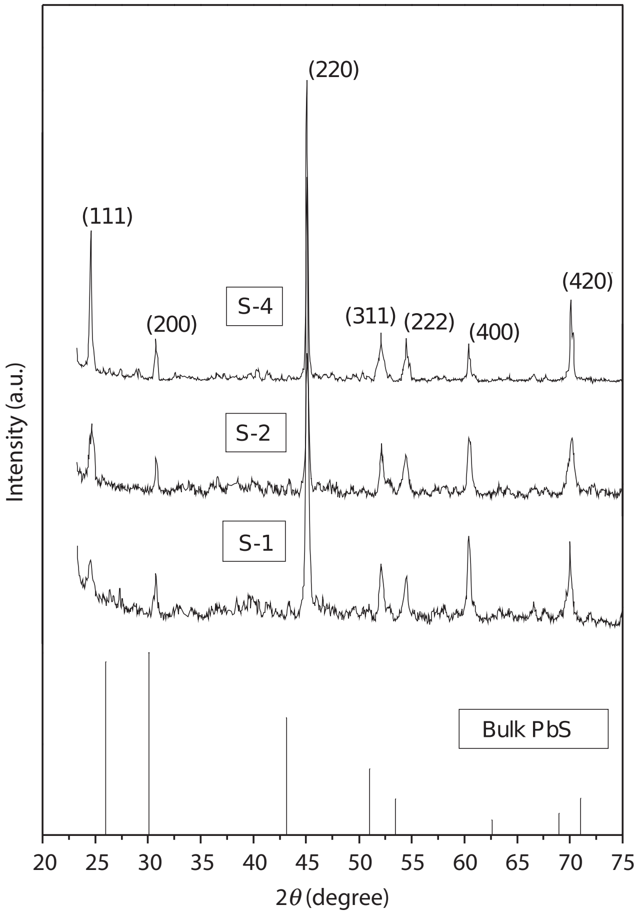

Figure 2. XRD spectra of PbS nanorods for undoped sample S-1 and silver-doped representative samples S-2 and S-4 along with the data obtained for bulk PbS from JCPDS data file.

as approximately 5.72%. The PbS lattice loses its cubic symmetry and transforms into a tetragonal one. The same can also be observed for silver-doped samples. It is also interesting to note that dopant concentration of silver in the nanorods is severely dependent on their size. The amount of silver incorporated into the PbS lattice decreases with the decrease in the size of nanorods, which is in consistent with the results obtained by Dalpian and Chelikowsky [16] for Mn-doped CdSe nanocrystals. They have shown that the stability of magnetic impurities is strongly size-dependent and that the formation energy of magnetic impurities increases with the reduction of nanocrystal size. The composition analysis of the doped samples obtained from the energy dispersive X-ray spectroscopy (EDS) profile is shown in Figure 3. The EDS measurements are carried out at different regions of each sample and are found to have uniform elemental compositions. The elemental percentage analysis obtained for samples shows the following compositions, sample S-2: Pb = 74.58, S = 22.81, Ag = 0.58; sample S-3: Pb = 76.02, S = 22.81, Ag = 1.17; and sample S-4: Pb = 77.32, S = 20.92, Ag = 1.76.

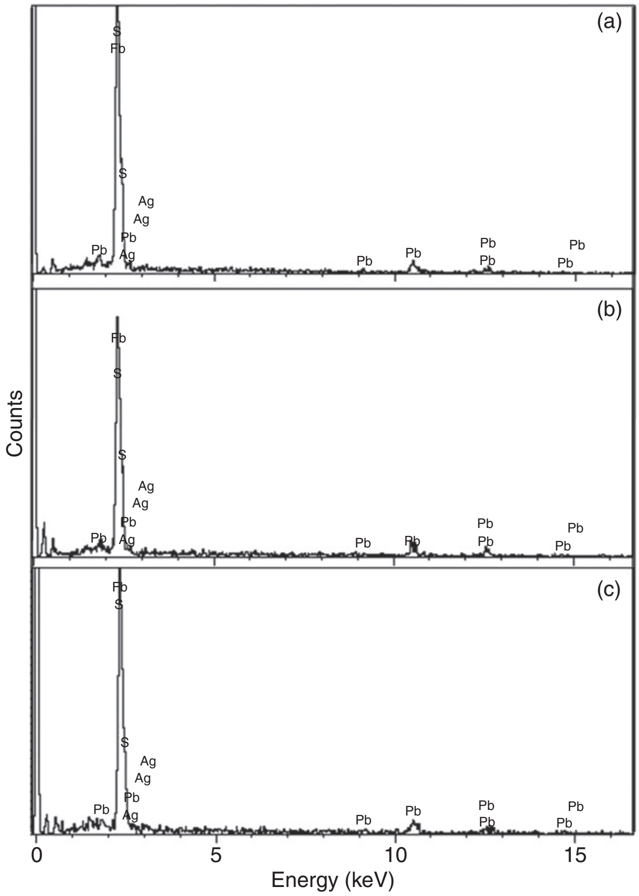

Figure 3. EDS profile (counts versus X-ray energy) showing the elemental compositions for the silver-doped samples (a) S-2, (b) S-3 and (c) S-4.

The identification of Ag in PbS host and their paramagnetic behaviours is obtained through the analysis of ESR spectra given in Figure 4 for all the silver-doped samples S2, S3 and S4, respectively. ESR measurements are carried out at 9.833 GHz at room temperature with a Bruker BioSpin GmbH spectrometer. With a judicious choice of modulation frequency (50–100 kHz) and modulation amplitude (10–15 Gauss), ESR signals are recorded without any appreciable spurious signals. The ESR signals are assigned to either silver atom Ag^0 ($4d^{10}5s^1$) and/or Ag^{2+} ($4d^9$) centre (Ag^+ being ESR inactive). The only signal observed for sample S-2 at 3510 Gauss is assigned to Ag^0 atoms. To maintain the charge neutrality of the PbS structure, only Ag^0 centres cannot be formed inside the PbS lattice; rather, they are residing at the PbS surface. This is further confirmed by the appearance of a broad surface plasmon resonance (SPR) band at approximately 420 nm as shown by the arrow mark in Figure 5. Such SPR band appears only for sample S-2 and not for samples S-3 and S-4. Adsorption of Ag^+ ions at the galena surface and their subsequent conversion into Ag^0 through ion-exchange reaction can be the plausible

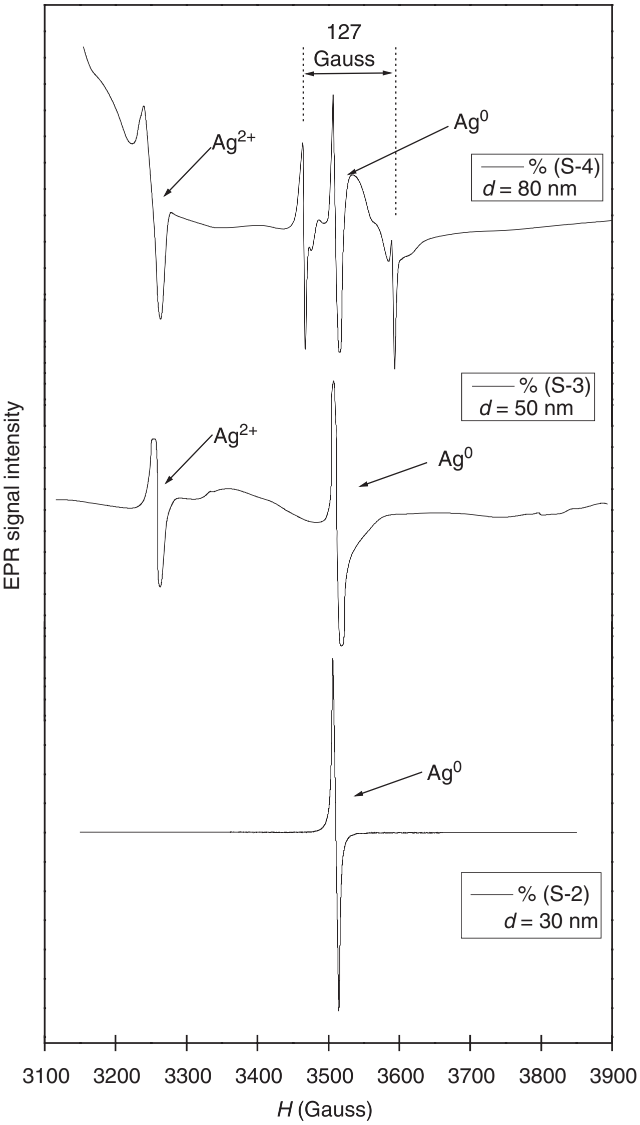

Figure 4. Room temperature ESR spectra of silver-doped samples S-2–S-4.

mechanism, as observed earlier by Scaini et al. [17]. In addition to the ESR signal for Ag^0, both the samples S-3 and S-4 exhibit another signal at approximately 3260 Gauss, which is attributed to the Ag^{2+} paramagnetic centres. Further, sample S-4 shows an additional splitting of the ESR signal due to Ag^{2+} centres with components asymmetrically located at approximately 3465 and 3592 Gauss, respectively. Now, substitution of Pb^{2+} by Ag^+ in the PbS lattice must be associated with the simultaneous creation of Ag^0 and Ag^{2+} centres to maintain the cation–anion ratio and charge the neutrality of the system. Creation of Pb^{2+} (hole) vacancies to act as a trap of Ag^+ ions and subsequent conversion into Ag^0 and Ag^{2+}

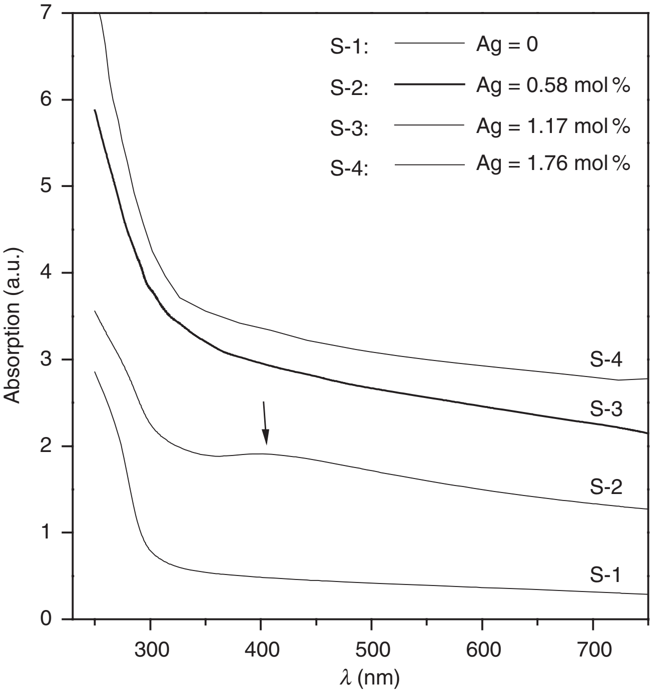

Figure 5. Optical absorption spectra for PbS nanorods for undoped sample S-1 and silver-doped samples S-2–S-4. The arrow mark indicates the position of the surface plasmon absorption band for sample S-2.

centres needs to be clarified to justify the ESR result. Creation of Ag^0 or Ag^{2+} centres through hole trapping at cation vacancies in doped, irradiated (by X-ray or by ultraviolet light) samples have been widely studied for various oxide and alkali-halide crystals by means of electron paramagnetic resonance [18–20]. The lattice distortions around the paramagnetic centres and the resulting crystal field splitting of ESR lines have led to many exciting theoretical and experimental investigations. In our case, we first look into the formation of Pb^{2+} vacancies in as-grown sample and subsequently into the crystallographic arrangements of atoms in PbS. PbS (galena) has the fcc cubic lattice with the octahedral coordination of Pb and S atoms. XRD data indicated that the strain-induced distortion of the lattice gives rise to a tetragonal structure. Ag^+ ions are supposed to be dissolved in a substitutional way and according to the reaction: substitutional ion → interstitial ion + vacancy. Silver occupies both the interstitial site as well as substitutional site of the lattice. Now the size of the substitutional Ag^+ ions (0.126 nm) is much smaller than the host Pb^{2+} ions (1.33 nm), more than a factor of 10. The mismatch in the size of the host and solute ions would therefore be expected to generate a large local strain within the lattice. This is true in both cases, whether an oversized ion replaces a smaller host ion or an undersized atom replaces a larger host ion. One would therefore expect a strain-induced binding of the Ag^+ ions into the cation vacancy. This large strain-induced binding energy therefore lowers the activation energy of diffusion significantly and it is further decreased with the increase in temperature. The vacancy binding energy is supposed to be proportional to the size difference of the Ag^+ and Pb^{2+} ions. The size difference of the solute and host ions determines the amount of strain generated on the host matrix and thereby controls the ability of the Ag^+ ions to capture vacancies. This clearly explains the substitution of Ag^+ ions into the PbS lattice for samples S-3 and S-4, which are grown at a relatively higher temperature of 80°C. Ag^{2+} ions are supposed to occupy the Pb^{2+} sites and Ag^0 atoms at the interstitial site of PbS lattice. Cowern et al. [21] have considered earlier the influence of strain on the Ge diffusion of Si and found an exponential increase of impurity diffusion with strain. The diffusivity in strained material (D') and in unstrained material (D) at temperature T is related by $D' = D \exp(-Qs/\mathrm{k}T)$, where Q is the dimension of energy per strain, s and k the observed strain and Boltzmann's constant, respectively.

The Ag^0 centres in sample S-2, responsible for the single symmetric ESR line at 3510 Gauss, is characterised by $g = 2.00234$, having a narrow line width of approximately 8 Gauss, respectively. The g value, approximately 2, further indicates weak spin-lattice coupling in the present system. Strong spin–lattice interaction and vibronic coupling to the optical E modes of vibration result in large broadening of the ESR spectra exhibited by d^9 ions (Cu^{2+}, Ag^{2+}, etc.) in the tetragonal cubic, Zn-chalcogenides and no observation of ESR spectra [22]. For sample S-2, no splitting due to hyperfine interactions with ^{107}Ag (51.8% abundance) and ^{109}Ag (48.2% abundance) isotopes is observed (each having a nuclear spin of $I = 1/2$). The nuclear gyromagnetic ratio for $^{107}Ag = 1.237 \times 10^{-4}$ and that of $^{109}Ag = 1.422 \times 10^{-4}$, respectively. The line width slightly increases to 12 Gauss for Ag^0 centres in sample S-3 without any change in g value. The line becomes complicated for sample S-4 with the appearance of two additional signals asymmetrically located on either side of the main signal at approximately 3510 Gauss. These two signals are separated by a field as large as approximately 127 Gauss. The line width of the main signal remains almost unchanged with respect to samples S-2 and S-3. The observation of (moderately intense) the asymmetric doublet with large field splitting is strong, indicative of the hyperfine interactions of ^{107}Ag and ^{109}Ag isotopes with $I = 1/2$. The doublet can be approximately characterised with a narrow line width, same as that of the main signal (10 Gauss) and having an intensity ratio consistent with that expected from the natural abundance of two isotopes. The lack of proper resolution of the doublet does not allow us to have a complete analysis, and indicate some g or A anisotropy. However, it can safely be concluded that splitting of Ag^0 inherits due to Breit–Rabi effect [23] rather than the presence of inequivalent silver atoms in the PbS lattice. Such asymmetric doublet is observed in the ESR spectrum from Sn centres in SiO_2 and is attributed to the case of strong hyperfine coupling [24].

4. Summary

In summary, we show here that in low-dimensional structures of PbS, in the form of nanorods, solid solubility of silver can be increased to approximately 1.74 mol%, quite higher than what is limited in bulk or natural galena. We also find that both Ag^0 and Ag^{2+} can stably coexist in PbS lattice. Lattice strain plays a crucial role for the creation of hole traps of Ag^+ ions and subsequent conversion of Ag^+ to Ag^0 and Ag^{2+} centres caused by thermodynamic processes to maintain the charge neutrality and stability of the system.

Acknowledgement

The authors acknowledge with thanks CSIR, Government of India, New Delhi, for providing financial support in carrying out this research work.

References

[1] H. Ohno, *Making nonmagnetic semiconductors ferromagnetic*, Science 281 (1998), pp. 951–956.

[2] F. Matsukura, H. Ohno, A. Shen, and Y. Sugawara, *Transport properties and origin of ferromagnetism in (Ga, Mn) As*, Phys. Rev. B 57 (1998), pp. R2037–R2040.

[3] S.J. Pearton, C.R. Abernathy, M.E. Overberg, G.T. Thaler, D.P. Norton, N. Theodoropoulou, A.F. Hebard, and Y.D. Park, *Wide band gap ferromagnetic semiconductors and oxides*, J. Appl. Phys. 93 (2003), pp. 1–13.

[4] P. Kacman, *Spin interactions in diluted magnetic semiconductors and magnetic semiconductor structures*, Semicond. Sci. Technol. 16 (2001), pp. R25–R39.

[5] D. Sanchez, A.H. MacDonald, and G. Platero, *Field-domain spintronics in magnetic semiconductor multiple quantum wells*, Phys. Rev. B 65 (2001), pp. 035301–10.

[6] T. Dietl, H. Ohno, and F. Matsukura, *Hole-mediated ferromagnetism in tetrahedrally coordinated semiconductors*, Phys. Rev. B 63 (2001), pp. 195205–21.

[7] H. Pascher, F. Geist, M. Kriechbaum, and N. Franck, *Heterostructures of dilute magnetic IV–VI compounds*, Phys. Scr. T 45 (1992), pp. 214–218.

[8] D.J. Priour and S. Das Sarma, *Clustering in disordered ferromagnets: The Curie temperature in diluted magnetic semiconductors*, Phys. Rev. B 73 (2006), pp. 165203–5.

[9] G. Giuli, E. Paris, Z. Wu, S.D. Panfilis, G. Pratesi, and G. Cipriani, *The structural role of Ag in galena (PbS). A XANES study*, Phys. Scr. T 115 (2005), pp. 387–389.

[10] H.J.K. Van Hook, *The ternary system* Ag_2S-Bi_2S_3-PbS, Econ. Geol. 55 (1960), pp. 759–788.

[11] T.G. Sharp and P.R. Buseck, *The distribution of Ag and Sb in galena; inclusions versus solid solution*, Am. Mineral. 78 (1993), pp. 85–95.

[12] A.N. Titov, I. Bryntse, S.G. Titova, and N.V. Toporova, *Silver intercalation in* $PbS_{1.18}(TiS_2)_n$, *n=1,2, misfit layer compounds*, Solid State Ionics 140 (2001), pp. 293–300.

[13] P.B. Barton and B.J. Skinner, *Geochemistry of Hydrothermal Ore Deposits*, Wiley, New York, 1979.

[14] P. Costagliola, F.D. Benedetto, M. Benvenuti, G.P. Bernardini, C. Cipriani, P.F. Lattanzi, and M. Romanelli, *Chemical specification of Ag in galena by EPR spectroscopy*, Am. Mineral. 88 (2003), pp. 1345–1350.

[15] A.R. Mandal and S.K. Mandal, *Polymer assisted preferential growth of PbS and PbS:Mn nanorods: Structural and optical properties*, J. Exp. Nanosci. 2 (2007), pp. 257–267.

[16] G.M. Dalpian and J.R. Chelikowsky, *Self-purification in semiconductor nanocrystals*, Phys. Rev. Lett. 96 (2006), pp. 226802–4.

[17] M.J. Scaini, G.M. Bancroft, and S.W. Knipe, *An XPS, AES, and SEM study of the interactions of gold and silver chloride species with PbS and* FeS_2*: Comparison to natural samples*, Geochim. Cosmochim. Acta 61 (1997), pp. 1223–1231.

[18] L.A. Boatner, R.W. Reynolds, M.M. Abraham, and Y. Chen, *Transition from static to dynamic Jahn–Teller effects as exhibited by the EPR spectra of* Ag^{2+} *in SrO, CaO, and MgO*, Phys. Rev. Lett. 31 (1973), pp. 7–10.

[19] G.E. Holmberg, W.P. Unruh, and R.J. Friauf, *An ESR and ENDOR study of the* Ag^0 *center in KCl and NaCl*, Phys. Rev. B 13 (1976), pp. 983–992.

[20] C. Kao, L.G. Rowan, and L.M. Slifkin, *EPR study of hole trapping at cation vacancies in silver halides*, Phys. Rev. B 42 (1990), pp. 3142–3151.

[21] N.E.B. Cowern, P.C. Zalm, P. van der Sluis, D.J. Gravestejin, and W.B. de Boer, *Diffusion in strained Si(Ge)*, Phys. Rev. Lett. 72 (1994), pp. 2585–2588.

[22] B. Clerjaud and A. Gélineau, *Strong spin-lattice coupling of Kramers doublets*, Phys. Rev. B 16 (1977), pp. 82–85.

[23] G. Breit and I.I. Rabi, *Measurement of nuclear spin*, Phys. Rev. 38 (1931), pp. 2082–2083.

[24] N. Chiodini, F. Meinardi, F. Morazzoni, A. Paleari, R. Scotti, and G. Spinolo, *Identification of Sn variants of the* $\acute{E}'$ *center in Sn-doped* SiO_2, Phys. Rev. B 58 (1998), pp. 9615–9618.